

Swimming in formation in krill (Euphausiacea), a hypothesis: dynamics of the flow field, properties of antennular sensor systems and a sensory–motor link

MUFTI P. PATRIA[†] AND KONRAD WIESE*

ZOOLOGISCHES INSTITUT UND ZOOLOGISCHES MUSEUM DER UNIVERSITÄT, MARTIN-LUTHER-KING-PLATZ 3, 20146 HAMBURG, GERMANY

[†]PRESENT ADDRESS: DEPARTMENT OF BIOLOGY, UNIVERSITY OF INDONESIA, FMIPA-UI, DEPOK 16424, INDONESIA

*CORRESPONDING AUTHOR: kwiese@zoologie.uni-hamburg.de

Received March 19, 2004; accepted in principle May 15, 2004; accepted for publication June 17, 2004; published online July 28, 2004

The act of swimming in formation by species such as Euphausia superba, Antarctic krill, is assumed to be regulated by a sensitivity to the characteristic and spatially elaborate flow field produced by this species of shrimp. We used a related species, Meganyctiphanes, North Atlantic krill, to visualize the flow field produced by tethered shrimps in an aquarium. In this situation, the propulsion jet flow some centimeters behind the shrimp is surrounded by a vortex ring of recoiling water motion from which, if the vortex is also produced by unrestrained swimming shrimp, a following shrimp hypothetically can draw forces of lift and propulsion to decrease energy expense in long-distance migration. Two antennular sensitivities to water vibration in frequency ranges 5–40 and 40–150 Hz were calibrated, and the activity of connected interneurons was traced into the abdominal pleopod-carrying segments. Water oscillation of 3–10 Hz frequency, applied to the antennules, was shown to entrain a closely synchronous pleopod beat in the stimulated specimens.

INTRODUCTION

Locomoting in formation is a behavior seen, e.g. in fish, birds and crustaceans [fish: (Weihs, 1975); birds: (Rayner, 1990); Crustacea, Euphausiacea: (Hamner *et al.*, 1983; Hamner, 1984; Strand and Hamner, 1990)], in species which in the three-dimensional space of air or water engage in long-distance migration. Formations are formed mainly to reduce energy expense in locomotion (Belyayev and Zuyev, 1969), but an ancillary benefit may result from the distraction of predators by a multitude of prey [sticklebacks fail more often to notice their predator, the kingfisher, when picking water fleas from a high-as compared with a low-density flock; (Milinski, 1984)].

Blinded fish can still swim in formation (Belyayev and Zuyev, 1969; Partridge and Pitcher, 1980), and the use of an echo sounder has shown that formations of Antarctic krill remain unchanged in structure in daylight and throughout the night (Everson and Bone, 1986a, b). Thus, a specific location and dynamic property in the

flow field, detected by antennular flow receptors, may enable individuals to maintain a constant position in a formation.

In the work presented here, we wanted to address the sensory aspects of movement in formation using the North Atlantic krill *Meganyctiphanes norvegica* [Fig. 1; (Mauchline, 1960; Frank and Widder, 1997; Onsrud and Kaartvedt, 1998; Tarling *et al.*, 1998; Spicer *et al.*, 1999; Fregin and Wiese, 2002)] because this close relative of *Euphausia superba* [swimming in formation: (Strand and Hamner, 1990 with earlier literature; Wiese and Ebina, 1995; Wiese, 1996)] swims by producing a propulsion jet of circular cross section generated by the metachronal beat of five pairs of swimmerets (Kils, 1982). Both euphausiid species are members of oceanic plankton, have a larger specific weight than that of water and have to swim continuously and hence generate their specific flow field continuously. The structure of formations of *E. superba* is characterized by an interindividual

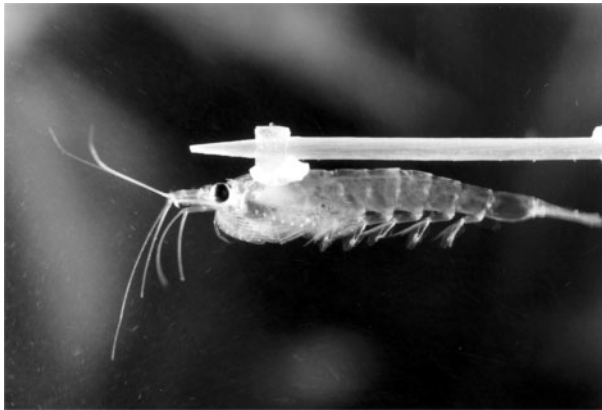


Fig. 1. *Meganyctiphanes norvegica*, North Atlantic Krill, tethered, in floating posture with pleopods stopped, startled by camera flash. Body length 45 mm plus 25 mm of antennular flagella extending forward. The filterbasket of thoracopods is folded up in swimming. The second antennae extend their flagella vertically downward.

distance of ~10–20 cm [inspection by diver: (Hamner, 1984; G. A. Tarling, personal communication)], which suggests that a specific orientation cue in the flow field is approximately that distance from the leading shrimp.

In this context, we wanted to measure the performance of the antennular flow sensor of *Meganyctiphanes*, because this highly complex sensory organ is expected to analyse a flow field, a task even nowadays a challenge for technical instrumentation.

Finally, we wanted to test the hypothesis that neighboring shrimps in the formation synchronize the beat of their pleopods (Hamner, 1984). The propulsion jet flow produced by the shrimp is modulated by the beat of swimmerets [*E. superba*, 3 Hz; *M. norvegica*, 6 Hz: (Wiese and Ebina, 1995)] and thus provides a rhythmic mechanosensory input to the antennules of following shrimps. Research on flight control in locusts by sensors of air flow (Gewecke, 1975; Horsemann *et al.*, 1983) suggests that mechanosensory interneurons conduct neural activity of antennular sensors to the neural motor pattern generators of the pleopods (*Procambarus*: Murchison *et al.*, 1993) in the abdominal segments of *Meganyctiphanes*. To find out, we recorded, in addition to the antennular sensory neurons, the activity of mechanosensory interneurons in the ventral nerve cord and the activity of pleopod muscle cells by advancing electrodes from outside the intact animal through pinholes in the skeleton.

MATERIALS AND METHODS

Meganyctiphanes norvegica (Sars, 1857), caught during daytime from the depths of Gulmarfjord, Sweden, were transferred to shore in thermos buckets (50 L, at 0°C) and stored in glass aquaria through which ran 8°C seawater from the

fjord. The aquaria were kept in a constant-temperature dark room. Food was provided in the evenings and consisted of minced *Mytilus* suspended in the aquarium.

Production of quantitatively described water oscillations

Quantitatively controlled water oscillations simulating aspects of turbulent flow were produced by a dipole source (van Bergeijk, 1967; Markl, 1983) that is a plastic sphere of 7 mm radius fastened to the end of an aluminum tube that moves axially, driven by a dynamic speaker system. Movements of the tube, maximally 250 μm peak to peak, were restricted to one axis by four thin steel wires tightened from the rim of the speaker basket to the aluminum tube. Artifact-free pulses of pure tone oscillations of defined rise time, frequency and amplitude were applied. Calibration was done by relating microscopically measured peak-to-peak oscillation of the sphere to peak-to-peak voltage fed into the coil of the speaker and repeating that procedure for each set of test frequencies. The thrust of the sphere produces a water movement in front of the sphere which attenuates along the extension of the axis of movement according to $1/r^3$, where r is distance of point of observation from the center of the sphere. In short, if r is set to two times the radius of the sphere (in our case a point 7 mm distant from the front of the sphere), the water movement is 1/8 of the peak-to-peak movement of the sphere (Wiese *et al.*, 1980). The oscillation amplitudes at the site of the receptors were calculated, not measured. The sphere movement was directed at a 90° angle toward the midpoint of the ventrally directed antennular flagellum. The distance from the front of the sphere to the flagellum was measured by a microscope. The volume of water which directly follows the movement of an object in water, without phase lag, is described as the near-field and is estimated at six times the volume of the moving object (Markl, 1983).

Including the sphere of 7 mm radius, this water mass occupies a spherical volume with radius 13.9 mm. Beyond this limit of the near-field, prediction is that the movements in the surrounding water mass develop phase lag with respect to the sphere movement.

Recording activity from the antennular nerves, ventral nerve cord and pleopod muscles

Glass microelectrodes of 5–15 M Ω resistance, filled with 3 M KCl, were used for recording neural and muscular activity. They were positioned from above onto the nerve through a small hole made by use of an insect pin. The basipodite of the antennule, the site of recording from the antennular nerve, was stabilized by a wire hook lowered from above. Recording of mechanosensory

interneurons of the ventral nerve cord was done through previously made holes in the ventral, totally transparent, cuticle of the intact animal. Small pinholes in the lateral part of abdominal tergites provided access for the microelectrode to unidentified muscles of the pleopod. The electrical activity of these muscles served as monitors of pleopod rhythm. Microelectrode amplifier and audiomonitor were conventional, and data were stored either using a RACAL 4 D (RACAL, Southampton, UK) instrumentation tape recorder or directly on a personal computer using the program SPIKE 2 (Cambridge Instruments, Cambridge, UK).

Establishing mechanosensory thresholds

The peak-to-peak movement of the sphere was decreased using calibration curves for a set of frequencies which relate the peak-to-peak voltage of the current through the speaker coil to the measured movement of the sphere when in water. For this study, the definition of threshold sensitivity was defined as the smallest sphere movement producing nerve activity that was still correlated to the stimulus, as judged by listening to the audiomonitor of the nerve recording. We estimated that this definition of threshold involved three to five action potentials produced in response to the stimulus.

Flow-field visualization

The method was generously provided to us by Thomas Breithaupt of Konstanz University and by Joseph Ayers of Northeastern University, Nahant, MA, USA (Breithaupt and Ayers, 1998). We established video protocols of the flow fields at Kristineberg at the Gulmarfjord so that we could use *Meganyctiphanes* specimens in optimal condition. Flow was visualized by light-reflecting particles (Acrylnitril-Butadien-Styrol: ABS, BAYER, Leverkusen, Germany) of 0.1 mm diameter and close to neutral buoyancy in seawater of 35 mil salinity (1.030 kg L^{-1}). Krill was tethered to swim in the center of the small side of an aquarium $35 \times 35 \times 50$ cm HWL (height, width, length) at ~ 4 cm below the water surface, 5 cm away from the pane and 17 cm distant from the side walls. The flow produced by *M. norvegica* is directed by the abdomen and tailfan as steep down as 45° . The positioning of the shrimp in the upper layer of the water mass was required to provide the maximum of the available space for the flow to develop. A projector and a slide with slit aperture produced a light sheet of 4 mm thickness extending through the water, oriented to coincide with the sagittal or horizontal plane of the tethered *Meganyctiphanes*, because the validity of the measurements depends on the particle trajectories being largely confined to the plane of illumination. The movement of the illuminated particles was recorded by S-VHS 625 Panasonic

Video-Camera. At Konstanz University, the recording was subsequently copied to a SONY EV-S9000E-PAL recorder and transferred into a Macintosh-Quadra computer by use of an AV-internal frame grabber card. The program COLORIMAGE (J. Ayers, internet communication; <http://www.neurotechnology.neu.edu/aboutcolorimage.html>) controlled the processing of data sets containing 25 pictures of videofilm taken per second. The program also produced the trajectories of selected particles and calculated the flow velocities.

RESULTS

Morphology of antennules and antennular sensitivity to water vibration in *Meganyctiphanes*

The antennules of *Meganyctiphanes* and of *Euphausia* typically have flagella of more than half the length of the body (Fig. 1), with the medial one articulated to move in a vertical plane and the lateral flagellum to move in a more horizontal plane (schematic representation of a frontal view: Fig. 2). If the shrimp swims fast, the flagella are actively extended to form a tighter bundle pointing forward. The flagella are fitted with both smooth and feathered hair-type sensilla, as shown by scanning electron microscopy (SEM) (Fig. 3a–e). Smooth sensilla of $\sim 50 \mu\text{m}$ length line the inner side of antennular flagella as shown

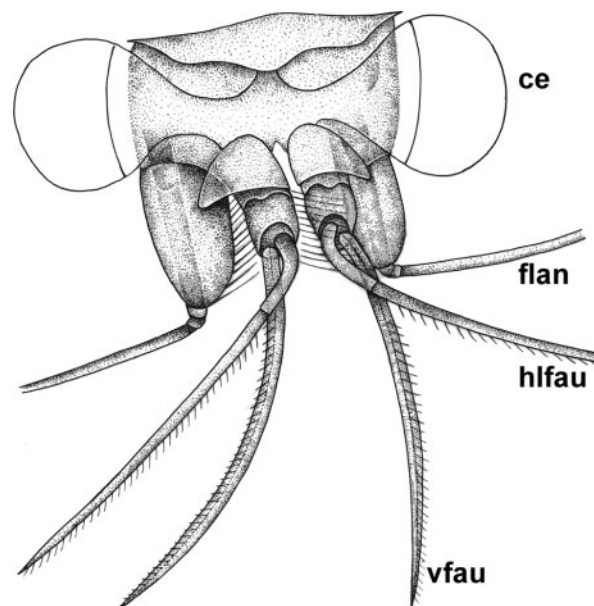


Fig. 2. View of the head section of *Meganyctiphanes* taken from a frontal slightly elevated position. The drawing shows the posture of horizontal laterally deflecting flagella of the antennules (**flau**), of ventrally directed flagella of antennule (**vfau**) and of the flagellum of the large second antenna (**flan**). The head section of *Meganyctiphanes norvegica* is dominated by the large compound eyes (**ce**).

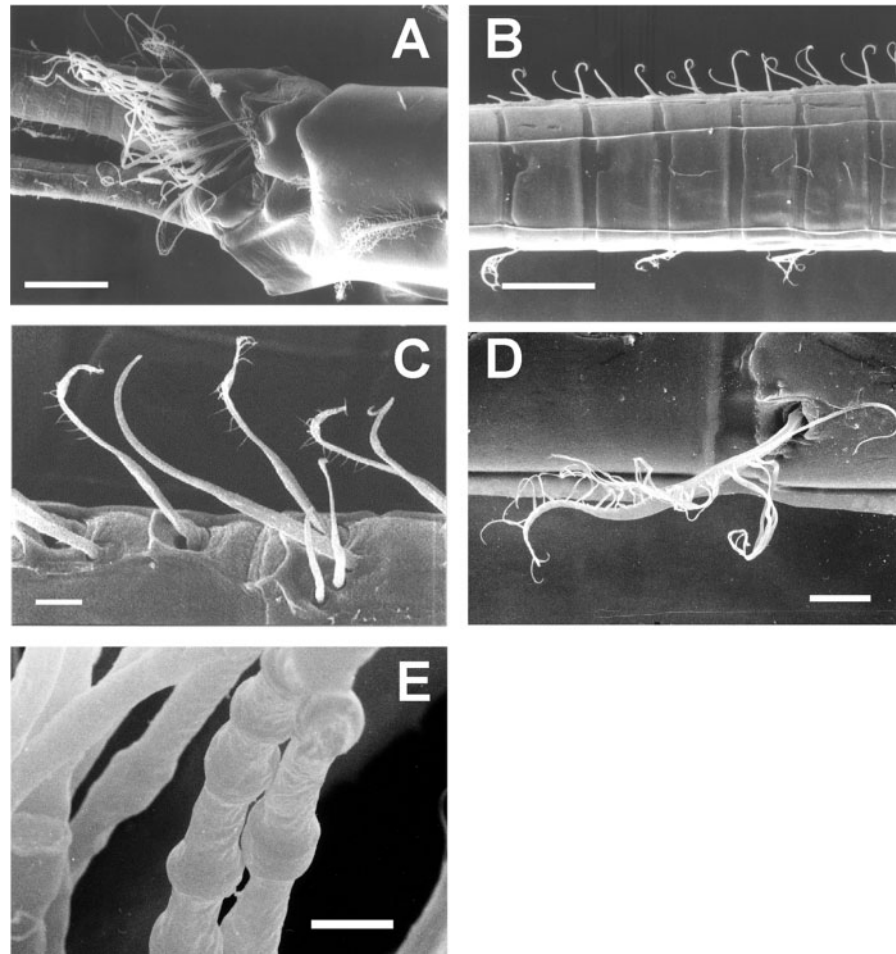


Fig. 3. Scanning electron microscopy (SEM) pictures of the antennular flagella of *Meganyctiphanes*. (a) The distal part of the antennular peduncle (basipodite) seen in lateral view; anterior is toward the left side, showing the tuft of aesthetascs (enlarged in panel e) and the bases of the two flagella, the upper the horizontally moving, the lower the vertically moving (see Fig. 2). (b) Section of the vertically moving flagellum showing the smooth hair-type sensilla on upper edge (enlarged in panel c) and the feathered (enlarged in panel d) hair-type sensilla at the lower edge. (e) Aesthetascs (chemoreceptors) have typically a beaded structure. Scale bars: a = 300 μm ; b = 100 μm ; c-e = 10 μm .

(Fig. 2 and 3b, top). The smooth sensilla, on average 3 per annulus, an estimated 200 annuli in all (Fig. 3c, enlarged), far outnumber the feathered sensilla, on average 1 per annulus (Fig. 3b, bottom; 3d, enlarged), which line the flagella at the outer side. Aesthetascs of beaded structure, assumed chemoreceptors (Fig. 3a and e), are positioned in a tuft at the distal end of the basipodite.

Antennular nerve activity was recorded by capillary microelectrodes through a pinhole in the basipodite. A dipole source (see *Materials and methods*) produced water oscillations of calculated peak-to-peak displacement. The movements were directed to be normal to the long axis of the flagellum which is hinged to move in a vertical plane and directed toward the midpoint.

At frequencies <40 Hz, relatively few sensory cells responded to the vibratory stimulus. In the extracellular recording, these cells were represented by larger action

potentials if compared with the responses of most of the cells to stimulus frequencies ≥ 40 Hz (Fig. 4a and b).

At water-oscillation frequencies 40, 80 and 100 Hz, responses are dominated by small-amplitude impulses occurring at high repetition rate. At 10 Hz oscillation frequency and suprathreshold stimulation, one or two impulses per sine cycle are observed.

The threshold curve of antennular sensitivity of *Meganyctiphanes* in response to calibrated water displacements at selected frequencies (Fig. 5) shows peak-to-peak displacements necessary at threshold (for definition see *Materials and methods*) of sensory-cell activation ranging from 10 μm at 5 Hz to 0.05 μm at 200 Hz.

The antennules of crustaceans and the antennas of insects are known as sensory organs for flow of the medium. Hence, a first assumption is that at threshold in all frequencies a uniform value of flow velocity

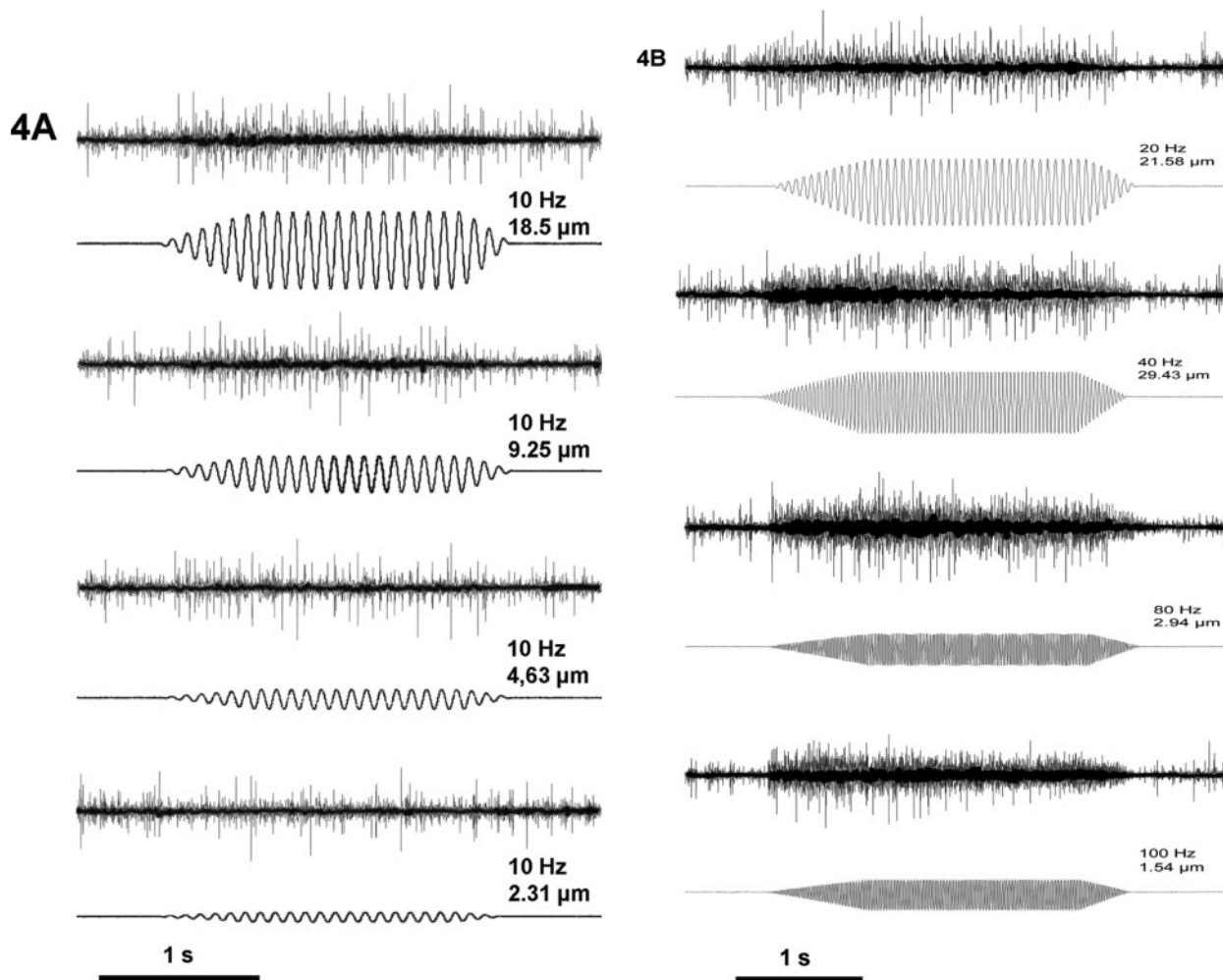


Fig. 4. (a) Few unit recording from the antennular nerve of *Meganyctiphanes*. Recordings at decreasing amplitude of water movement. Values of water movement amplitude were obtained by calculation (see *Materials and methods*). The stimulus trace is the alternating voltage fed into the speaker coil driving the dipole sphere. At frequencies <40 Hz, the sensory-cell activity originates from the proprioceptors of the basal hinge of the flagellum. (b) Sample recordings at a series of increasing frequencies. No 1:1 responses are visible in the recordings at 40, 80 and 100 Hz. The sensory-cell activity at these frequencies is attributed to the smooth-hair-type sensilla lining the anteriorly pointing edge of the antennular flagella.

prevails, differing in particle-displacement amplitude at different frequencies ($v = d \times 2\pi f$, where v is velocity, d is displacement and b is acceleration). The dotted isovelocity line in Fig. 5, set *ad libitum* to 0.5 mm s^{-1} , allows comparison of the measured thresholds for the mentioned ideal characteristic of a true flow sensor. In the frequency range 5–40 Hz, the displacements at threshold follow the dotted line more or less in parallel. And in fact, velocities at threshold are 0.25 mm s^{-1} at 5 Hz, 0.31 mm s^{-1} at 20 Hz and 0.25 mm s^{-1} at 40 Hz. In the range of frequencies tested >40 Hz, however, the threshold curve changes to another, more negative slope, indicating that a sensor system adhering more to the parameter of acceleration [$b = d \times (2\pi f)^2$] provides the sensitivity in this frequency range (cf. Wiese and

Marschall, 1990). The acceleration at threshold in this frequency range was found to be 7.5 cm s^{-2} at 80 Hz, resp. 7.8 cm s^{-2} at 200 Hz.

Two sensory organs come to mind which potentially play a role here: the proprioceptor at the base of the respective flagellum [*Euphausia*: (Wiese and Marschall, 1990); *Panulirus*: (Wyse and Maynard, 1965); *Cherax*: (Sandeman, 1985)] and the large number of smooth hair-type sensilla on the annuli of the flagellum. Correspondingly, hair-type sensilla or flagellar hinge were blocked by glue, the hinge was rhythmically flexed and extended and finally a wire loop sliding along the flagellum was employed. The preliminary experience that the wire sliding along the flagellum evoked large numbers of preferentially small-size action potentials

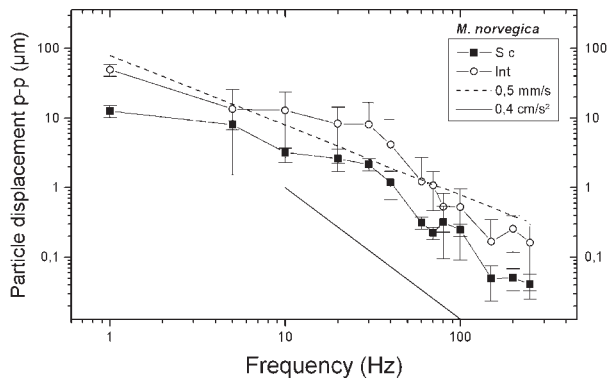


Fig. 5. Measurement of thresholds of response to water vibration of sensory cells (Sc) recorded in the antennula and in interneurons (Int) of the abdominal ventral nerve cord of *Meganyctiphanes norvegica*. The dotted line with slope -1 represents an isovelocity line of particle flow of 0.5 mm s^{-1} . The threshold curve (based on $N = 32$ animals recorded from) is drawn using the means of threshold values obtained and \pm standard deviations. The curve indicates two receptor systems at work. In the frequency range $5\text{--}40 \text{ Hz}$, a receptor system is tuned to velocity with a characteristic threshold of 0.25 mm s^{-1} . At frequencies $40\text{--}100 \text{ Hz}$, another receptor system is tuned to acceleration with a characteristic threshold value of 7.5 cm s^{-2} . The solid line with slope -2 is an isoacceleration line.

points at the small and smooth hair-type sensilla lining the length of the flagellum likely responsible for providing the sensitivity to water vibration at frequencies $>40 \text{ Hz}$. The proprioceptors of the hinge at the base of the flagellum likely need the larger water displacements at $5\text{--}40 \text{ Hz}$ to receive a suprathreshold stimulus.

Response of interneurons of the ventral nerve cord to water vibration

Microelectrodes were advanced from outside the intact animal through a pinhole in the transparent skeleton into the ventral nerve cord. The two frequency ranges (more velocity-dependent in the frequency range $<40 \text{ Hz}$ and more acceleration-dependent in the frequency range $>40 \text{ Hz}$) of sensitivity observed in sensory-cell activity are also evident in the thresholds of interneurons (Fig. 5). The displacements at the threshold of activation of the interneurons were generally larger than those measured in the antennular sensory cells. The site of recording of the ventral nerve cord interneurons, the first abdominal segment, is apparently capable of contacting the motor pattern generator circuits (Murchison *et al.*, 1993) of pleopod (swimmeret) action.

The neural pattern generators for pleopod movement are entrained by the rhythm of patterned nerve activity descending from the antennules

A synchronization of pleopod movement among a leading and a following animal in the formation, as pre-

viously assumed (Hamner, 1984), requires that the activity of the antennular flow sensors result in pace-setting input to the neural motor pattern generator circuits of pleopod action. *Meganyctiphanes* in general uses a 6 Hz rhythm of pleopod movement (Wiese and Ebina, 1995). During faster spurts, the frequency is raised to near 10 Hz or at other times may be lowered to as low as 4 or 3 Hz . Within the range of these frequencies of pleopod movement, we stimulated the antennular flagella with low-frequency water oscillations produced by the dipole source (Fig. 6a). Simultaneously, the rhythm of the pleopod movement was monitored by myograms recorded from an unidentified group of muscles of the coxopodite of one of the pleopods (Fig. 6b, top trace). The large pulses in the center group of activity likely are additional muscle activity in response to the very strong antennular activity in the lower trace. At very low stimulus frequencies, the pleopod pace changed and locked into twice the frequency of the stimulus, whereas at $6\text{--}10 \text{ Hz}$ of stimulation, the pleopod movement followed one to one the cycles of water motion. Critical inspection of the recordings shows that synchronization is not complete, i.e. the motor pattern generator of *Meganyctiphanes* has maintained some degree of independence in the stimulus situation provided.

The propulsion jet flow produced by *Meganyctiphanes* gives rise to a ring-shaped vortex in which flow direction reverses

The pleopods of tethered swimming *Meganyctiphanes* produce a jet flow of about 10 cm s^{-1} at the tip of the swimmerets. Such isolated jet flows of circular cross section (Schlichting, 1982) attenuate according to the rule of thumb $1/x$, where x (cm) is the distance of the point of observation from the origin of the jet flow. The attenuation results from friction with the resting water body, which results in vortices of recoiling water from the mantle of jet flow. At 20 cm distance from the tip of the pleopods, the movement of light-reflecting particles is still suitable for macroscopic video protocol (Fig. 7a, c and d). The whole flow field of interest thus appears to fit into a $35 \times 35 \times 50 \text{ cm}$ HWL aquarium. This size is experimentally advantageous, nevertheless a compromise, because only a much larger tank definitely excludes interactions of the developing flow field with the walls of the tank.

Only suspended particles within a 4-mm -thick sheet of water in parallel to the sagittal plane of the shrimp's body and in the plane of the jet flow are illuminated to have negligible velocity in a direction normal to most of particle movement. The visualization was composed of blocks of data with 25 frames s^{-1} . It shows that a comparably small diameter of the jet flow near the origin

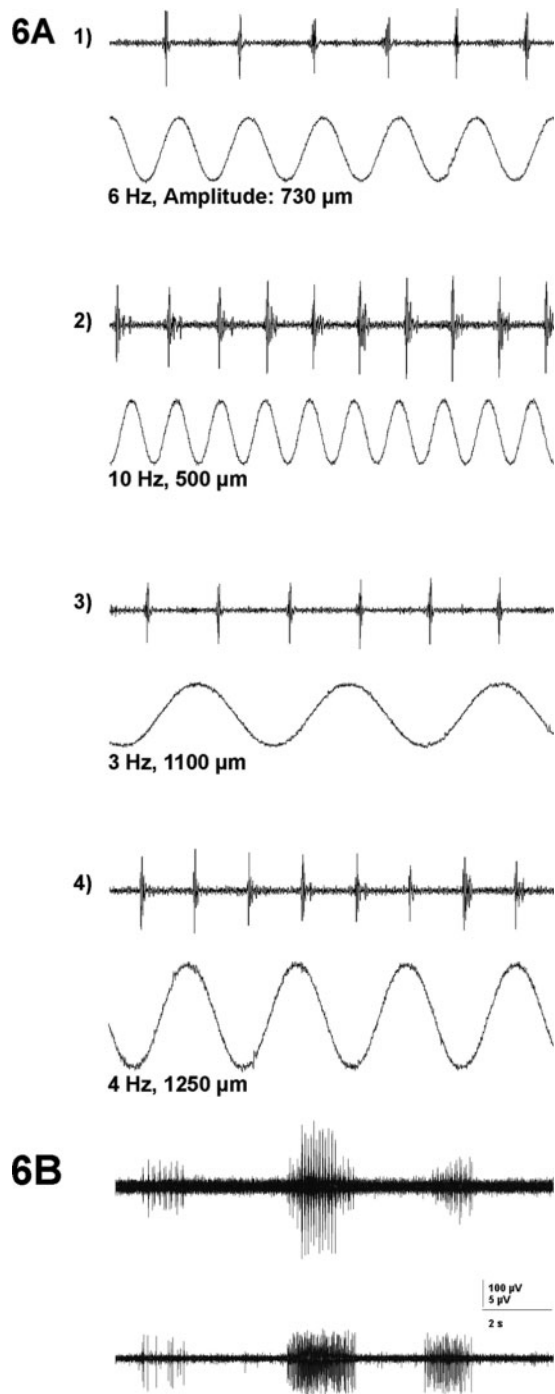


Fig 6. (a) The rhythm of swimmerets (pleopods) of *Meganyctiphanes* is monitored [(1)–(4)] by myograms from swimmeret muscles at top trace, while different frequencies of water vibration, lower trace (alternating voltage fed to the speaker driving the dipole source), are applied to the antennular flagella. The beat of pleopods is regularly ~ 6 Hz (1). At frequencies < 6 Hz in (3) and (4), the pleopods close to synchronize to twice the frequency of the vibration applied to the antennule; vibration of 10 Hz at maximum accelerates the pace of pleopods to even 10 Hz; see (2). (b) Antennular nerve activity (lower trace) and correlated activity in pleopod muscles (upper trace) in response to three different stimuli of water vibration of different intensity generated by a hand-held probe.

widens with distance from the pleopods of the shrimp. The distance between white dots in line is the movement of the particle during 40 ms of delay between frames. Vortices of reversing water motion above and below the jet appear at ~ 8 – 10 cm from the origin of the jet. These vortices show not only in the vertical plane but also in the visualization in the horizontal plane (Fig. 7c), extending through the shrimp's body and through the axis of the jet flow, to the right and left.

Visibility in two orthogonal planes (Fig. 7a, c and d) shows the vortices to be cross sections of a vortex ring surrounding the axis of the jet. Water from the jet is accelerated into reversing water rotation by the friction between jet flow and resting water.

At the end of the first 180° of the vortex, the direction of water motion has changed from parallel to the driving jet to exactly the opposite direction. At the apex of the vortex ring above the driving jet flow, the reversing water movement comprises a component of upward- and forward-directed water motion. A properly positioned *Meganyctiphanes* could profit from components of lift and propulsion available at phases from 90° to an estimated 150° with respect to the onset (axis of jet flow) of the circular motion. A reviewer of this manuscript criticized that the vortex ring would show only in restrained swimming shrimp, not in unrestrained, and that the vortex ring could also be the effect of water returning along the walls of the aquarium to the pleopods, in short could be a result of too small an aquarium. Points in defense of the existence of the observed vortex ring even in unrestrained swimming shrimps will be made in the discussion.

DISCUSSION

The measurements reported above were taken during expeditions to Kristineberg's Marina Forskningsstation at the Gulmarfjord in southwest Sweden. Correspondingly, they lack some desirable details such as more flow-field visualization and more electrophysiology. However, they are certainly suited to guide further work.

The measurements have documented a dynamic property of the flow field produced by swimming *Meganyctiphanes* which, pending more detailed proof of the existence in unrestrained swimming shrimp, is crucial to swimming in formation. The measurements have provided the specification of two of the sensor systems used by *Meganyctiphanes* in flow-field analysis. The two sensor systems, by connected mechanosensory ventral cord interneurons, are able to entrain the pleopod rhythm. Thus, a sensory-motor reflex-link from antennules to pleopod motor system exists, with the consequence that a continued pattern of synchronized flow fields is to be expected, extending from individual to

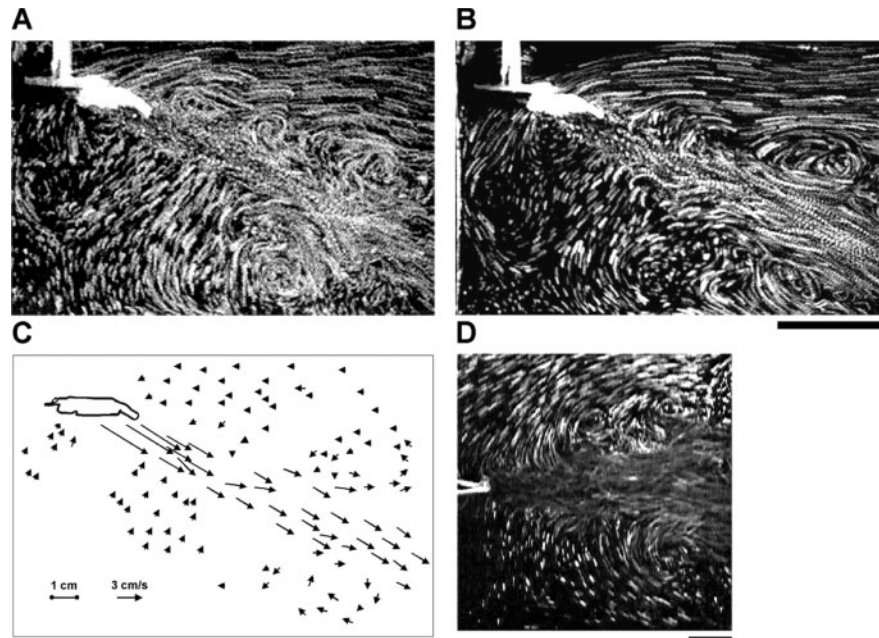


Fig 7. Flow-field visualization by movement of light-reflecting particles in an illuminated sheet (see *Materials and methods*) of water parallel to the sagittal (**a, b**) and an orthogonal to that, a more horizontal (**d**) plane through the tetheredly swimming shrimp and the generated jet flow. Please remember that the right border of pictures shown in panels a, b and d does not coincide with the backside wall of the tank, as the camera has taken only a detail of the flow field. (a) The shrimp, ~45 mm in body length, serves as calibration to show that ~8–10 cm distant from the tip of the tail a vortex has developed below and above, right and left of the propulsion jet in which (holds for the section above the jet) water moves upward and forward, as displayed in panel **c**, where visualization shown in panel a has been analysed by computer. (d) In a more horizontally arranged light sheet, tilted slightly downward toward the posterior of the shrimp, vortices right and left of the jet flow are apparent. Vortices observed in two orthogonal planes of the water body strongly suggest that the vortex has the shape of a ring and an estimated diameter of ~7 cm. (b) In another visualization of the sagittal plane, this vortex shows again at 8–10 cm distance behind the tetheredly swimming shrimp. Scale bars: b = 4 cm, holds also for a; d = 2 cm.

individual throughout the formation. Reference to earlier work is now used to comment on the observations.

The flow field produced by swimming *Meganyctiphanes*

The five pairs of metachronally beating swimmerets of *Meganyctiphanes* produce a propulsion jet flow of circular cross section (Kils, 1982), contrasting sharply to the flows produced by swimming fish (Stamhuis and Videler, 1995; Mueller *et al.*, 1997; Hanke *et al.*, 2000). The jet propulsion used by euphausiids (for a most recent study see Yen *et al.*, 2003) is relatively unique (except for some pelagic isopods) and not at all uniform across all shrimps using their pleopods in locomotion. For example, the sand shrimp *Crangon crangon*, an inhabitant of fast-moving tidal currents, uses the swimmerets more like oars which generate only local turbulence while accelerating the animal (K. Wiese, personal observation).

The particular advantage of producing propulsion by jet flow is still undisclosed. *Euphausia superba* and *Meganyctiphanes* are long-distance diel vertical [>100 m; (Mauchline, 1960; Frank and Widder, 1997)] and/or seasonal migrators (Everson and Bone, 1986a) and likely use the most

economic ways to locomote. On the other hand, they may use the characteristically modulated flow signal [the spectrum contains a fundamental (*E. superba*, 3 Hz; *M. norvegica*, 6 Hz) and three harmonics (Wiese and Ebina, 1995)] for close-range communication of their presence to conspecifics in the continuous darkness in which they live. Recent measurement of the lifetime of characteristic frequencies in the wake of swimming *Euphausia* and *Metapenaeus* (Ebina and Miki, 1996) has revealed that these frequencies are detectable at 40 cm behind the shrimp. This suggests that characteristic flow signals of shrimp probably are essential means to assemble the scattered swimming and feeding shrimps into denser clusters.

The flow field produced by the unrestrained swimming shrimp may be different from that produced by a tethered shrimp, however, not different in the essential quality for the following reason. The jet flow produced by the swimming shrimp will always be faster than the resulting forward movement of the shrimp, because of the resistance which counteracts the movement. Moreover, divers (Hamner, 1984) have reported that *Euphausia* swimming in formation use all their force in swimming, thus generating a strong propulsion jet.

The reverting vortex of water movement (Fig. 7b) which surrounds the jet completely is a result of friction between fast moving jet and resting water (Karman vortex: Denny, 1988). According to this author, such vortices surround all free jets of circular cross section, depending, of course, on the speed of the jet flow. Yen *et al.* (Yen *et al.*, 2003) have, by technically advanced methods, observed and measured positive and negative vorticity above and below the jet flow produced by the swimmerets of *Euphausia pacifica*. This species is only 20 mm in size and thus produces weaker jet flow. The two flow-field visualizations in *M. norvegica* and in *E. pacifica* are at present hard to compare because Yen *et al.* (Yen *et al.*, 2003) have provided only processed flow fields and no original enlarged video frames.

The aquarium in which we made the visualizations was 50 cm long. The video camera, however, was focused only onto the area next to the swimming shrimp. Hence, the right side rim of Fig. 7a–d does not represent the backside wall of the tank which of course will later reflect the jet flow. The wall as reflector is not the cause of the reversion vortex as seen in Fig. 7a and b: two vortices are seen above the jet flow, one behind the other. If the last vortex was generated by the reflection of the jet, the first vortex required another explanation.

Pending better experimental proof, it has to be pointed out that at the apex of the vortex ring the water particles in the vortex move upward and forward before turning into close circulation. The upward- and forward-directed components of water flow in the cross section of the vortex represent forces of lift and propulsion which help a shrimp positioned there to maintain its position with respect to the shrimp it trails. Similar effects influence bird migration performance, as summarized by Rayner (Rayner, 1990).

Antennules and antennas as sensors relevant in formation swimming

Sensors designed to measure medium flow characteristically show a more or less constant value of velocity (calculated as: $v = d \times 2\pi f$) at threshold throughout a range of frequencies of water vibration (Fig. 5, left side; frequency range 5–40 Hz). Adherence of the sensor system to the component of acceleration of medium movement [calculated as: $b = d \times (2\pi f)^2$] is indicated in the frequency range >40 Hz by the steeper negative slope of the measured threshold curve (Fig. 5, right side; frequency range 40–100 Hz).

The measured sensitivity of antennular receptors to a flow of 0.25 mm s^{-1} at 40 Hz and at 10 Hz is representative of the range 5–40 Hz. This value is slightly less sensitive if compared to the velocity thresholds measured in *E. superba* of 0.15 mm s^{-1} in the same frequency range

(Wiese and Marschall, 1990). Though 32 *M. norvegica* were measured in establishing this threshold, a side-by-side measurement of the two species of shrimps would be required to prove the difference in thresholds – a genuine fact. On the other hand, the sensitivity in the antennules of *M. norvegica* is sufficient to measure water vibration and flow field at 8–10 cm distance from the origin of the jet flow, at the site of the vortex ring where flow has slowed down to an estimated 1 cm s^{-1} .

When swimming, *Meganyctiphanes* holds the large second antenna tilted back and sideways downward. In this posture, the antennas should be able to detect the apex of a vortex ring surrounding the jet flow produced by a shrimp swimming ahead. Breithaupt and Tautz (Breithaupt and Tautz, 1990) have identified the antenna of crustacea as a sense organ for touch.

Antennular activity in response to water vibration close to synchronizes the beat of swimmerets

The abdominal ventral nerve cord of *M. norvegica* was found to contain descending interneurons activated by water vibration applied to the antennules. This result is reminiscent of results from studies demonstrating that the control of locust flight is mediated by flow sensors including proprioceptors of the wing and the antenna and hair-type sensors of the head (Gewecke, 1975; Horsmann *et al.*, 1983; Möhl and Bacon, 1983). The essence of this work was that the flow sensors have a very strong influence on the neural pattern generation for wing movement, a circuitry not yet identified at the cellular level. The neural pattern generator for crustacean pleopod movement on the other hand has been extensively studied in crayfish (Murchison *et al.*, 1993; Tschuluun *et al.*, 2001), and a transfer of our observations made on the constantly swimming *M. norvegica* might trigger new experiments on the neural control of pleopod action.

We applied water vibration to the antennules to simulate a component of the water oscillations of the flow field which act on the antennules of a shrimp when swimming in formation. Myograms of an unidentified pleopod muscle showed remarkable success of the vibrating sphere in entraining the rhythm of pleopod beat using a set of selected water oscillations. Small shifts in phase relation between sphere movement and pleopod muscle activity indicated that the antennular sensory activity modulates a central pattern generator and has not taken total control of the pleopod rhythm. This observation explains the ease with which the central pattern generator is able to change from one-to-one relation of oscillation and muscular response to the mode of one oscillation relating to two bursts of muscular activity at stimulus frequencies 3 and 4 Hz (Fig. 6a).

The mechanosensory interneurons measured while tracing the neural activity evoked in the antennules throughout the ventral nerve cord were distinctly less sensitive than the antennular receptor cells (Fig. 5). Our interpretation of this result is that a presumed existing lateral inhibitory network between the two antennular inputs could have lowered the sensitivity of the pathway by precurrent lateral inhibition in a situation of common mode stimulation (Wiese and Schultz, 1982; Reichert *et al.*, 1983).

The evidence that the beat of pleopods synchronizes to a frequency of water vibration applied to the antennules (Fig. 6a) is not devaluated by the fact that the synchronization works only in a very limited range of frequencies. The large load of water, the complicated folding and unfolding of the pleopods for return- and powerstroke and the metachrony (Kils, 1982) of movement of five pairs of swimmerets probably all provide rigid limitations to the range of frequencies in which the entrainment is observed.

From the facts discussed above, the synchronous beating of swimmerets among leader and follower likely is a corollary to swimming in formation. Identical size of members of the formation, as reported by divers (Hamner, 1984), fits well into the picture. As a consequence, disturbance at the front edge of the formation would be expected to propagate at high speed as individuals react to signals from shrimp ahead of them. The actual trajectories of individual euphausiids in formation during a disturbance should be recorded and analysed to understand yet another case of complicated communication.

ACKNOWLEDGEMENTS

The authors thank Kristineberg's Marina Forskningsstation, Kristineberg, Gulmarfjord, Sweden for hospitality and steady support as well as for extending to us financial help by the program Access to Research Institutions (ARI) of the EU commission. Thanks also to Torsten Fregin and Monika Hänel from the Zoology Department at Hamburg, who expertly helped in processing the figures and made the drawing of the head section of *M. norvegica*, respectively.

REFERENCES

Belyayev, V. V. and Zuyev, G. V. (1969) Hydrodynamic hypothesis of school formation in fishes. *Probl. Ichthyol.*, **9**, 578–584.

van Bergeijk, W., (1967) Introductory comments on lateral line function. In Cahn, P. (ed.), *Lateral Line Detectors*. Indiana University Press, Bloomington, IN, pp. 73–81.

Breithaupt, T. and Ayers, J. (1998) Visualization and quantification of biological flow fields through video-based digital motion-analysis techniques. *Mar. Freshw. Behav. Physiol.*, **31**, 55–61.

Breithaupt, T. and Tautz, J. (1990) The sensitivity of crayfish mechanoreceptors to hydrodynamic and acoustic stimuli. In Wiese, K. *et al.* (eds), *Frontiers in Crustacean Neurobiology*. Birkhäuser, Basel, pp. 114–120.

Denny, M. W. (1988) *Biology and the Mechanics of the Wave Swept Environment*. Princeton University Press, Princeton, NJ.

Ebina, Y. and Miki, T. (1995/96) Range and biological significance of characteristic water currents produced by the shrimp *Euphausia superba* and *Metapenaeus intermedius*. *Zoology*, **99**, 163–174.

Everson, I. and Bone, D. G. (1986a) Detection of krill (*Euphausia superba*) near the sea surface: preliminary results using a towed upward looking echo sounder. *Br. Antartct. Surv. Bull.*, **72**, 61–70.

Everson, I. and Bone, D. G. (1986b) Effectiveness of the RMT 8 system for sampling krill (*Euphausia superba*) swarms. *Polar Biol.*, **6**, 83–90.

Frank, T. M. and Widder, E. A. (1997) The correlation of downwelling irradiance and staggered vertical migration patterns of zooplankton in Wilkinson Basin, Gulf of Maine. *J. Plankton Res.*, **19**, 1975–1991.

Fregin, T. and Wiese, K. (2002) The photophores of *Meganctiphanes norvegica* (M.Sars) (Euphausiacea): Mode of operation. *Helgol. Mar. Res.*, **56**, 112–124.

Gewecke, M. (1975) The influence of the air-current sense organs on the flight behaviour of *Locusta migratoria*. *J. Comp. Physiol.*, **103**, 79–95.

Hamner, W. M. (1984) Aspects of schooling in *Euphausia superba*. *J. Crustac. Biol.*, **4**, 67–74.

Hamner, W. M., Hamner, P. P., Strand, S. W. *et al.* (1983) Behavior of Antarctic krill *Euphausia superba*: Chemoreception, feeding, schooling and molting. *Science*, **220**, 433–435.

Hanke, W., Brücker, C. and Bleckmann, H. (2000) The ageing of the low-frequency water disturbances caused by swimming goldfish and its possible relevance to prey detection. *J. Exp. Biol.*, **203**, 1193–1200.

Horsemann, U., Heinzel, G. and Wendler, G. (1983) The phasic influence of self generated air-current modulations on the locust flight motor. *J. Comp. Physiol.*, **150**, 427–438.

Kils, U. (1982) The swimming behaviour, swimming performance and energy balance of Antarctic krill, *Euphausia superba*. *Biomass Sci. Res. Ser.*, **3**, 1–121.

Markl, H. (1983) Vibrational communication. In Huber, F. and Markl, H. (eds), *Neuroethology and Behavioural Physiology*. Springer, Berlin/Heidelberg/New York, pp. 332–353.

Mauchline, J. (1960) The biology of the euphausiid *Meganctiphanes norvegica* (M.Sars). *Proc. R. Soc. Edinb.*, **67B**, 141–179.

Milinski, M. (1984) A predator's cost of overcoming the confusion effect of swarming prey. *Anim. Behav.*, **32**, 1157–1162.

Möhl, B. and Bacon, J. (1983) The tritocerebral commissure giant (TCG) wind-sensitive interneurone in the locust. II. Directional sensitivity and role in flight stabilisation. *J. Comp. Physiol.*, **150**, 453–465.

Mueller, U. K., van den Huevel, B. L. E. and Stamhuis, E. J. (1997) Fish footprints: Morphology and energetics of the wake behind a continuously swimming mullet (*Chelon labrosus* Risso). *J. Exp. Biol.*, **200**, 2893–2906.

Murchison, D., Chrachri, A. and Mulloney, B. (1993) A separate local pattern-generating circuit controls the movement of each swimmeret of crayfish. *J. Neurophysiol.*, **70**, 2620–2631.

Onsrud, M. S. R. and Kaartvedt, S. (1998) Diel vertical migration of krill *Meganctiphanes norvegica* in relation to physical environment, food and predators. *Mar. Ecol. Prog. Ser.*, **171**, 209–219.

- Partridge, B. L. and Pitcher, T. J. (1980) The sensory basis of fish schools: relative roles of lateral line and vision. *J. Comp. Physiol.*, **135**, 315–325.
- Rayner, J. M. V. (1990) The mechanics of flight and bird migration performance. In Gwinner, E. (ed.), *Bird Migration: Physiology and Ecophysiology*. Springer, Berlin, pp. 283–299.
- Reichert, H., Plummer, M. R. and Wine, J. J. (1983) Identified local non-spiking interneurons mediate nonrecurrent lateral inhibition of crayfish mechanosensory interneurons. *J. Comp. Physiol. A*, **151**, 261–273.
- Sandeman, D. C. (1985) Crayfish antennae as tactile organs: their mobility and the response of their proprioceptors to displacement. *J. Comp. Physiol.*, **157**, 363–373.
- Schlichting, H. (1982) *Grenzschicht-Theorie*. 8. Aufl. Verlag G. Braun, Karlsruhe, 754 pp.
- Spicer, J. I., Thomasson, M. A. and Stroemberg, J. O. (1999) Possessing a poor anaerobic capacity does not prevent the diel vertical migration of Nordic krill *Meganyctiphanes norvegica* into hypoxic waters. *Mar. Ecol. Prog. Ser.*, **185**, 181–187.
- Stamhuis, E. J. and Videler, J. J. (1995) Quantitative flow analysis around aquatic animals using laser sheet particle image velocimetry. *J. Exp. Biol.*, **198**, 283–294.
- Strand, S. W. and Hamner, W. M. (1990) Schooling behavior of Antarctic krill (*Euphausia superba*) in laboratory aquaria: reactions to chemical and visual stimuli. *Mar. Biol.*, **106**, 355–359.
- Tarling, G. A., Matthews, J. B. L., Saborowski, R. et al. (1998) Vertical migratory behaviour of the euphausiid, *Meganyctiphanes norvegica*, and its dispersion in the Kattegat Channel. *Hydrobiologia* **375/376**, 331–341.
- Tschuluun, N., Hall, W. and Mulloney, B. (2001) Limb movements during locomotion: Tests of a model of an intersegmental coordinating circuit. *J. Neurosci.*, **21**, 7859–7869.
- Weihs, D. (1975) Some hydrodynamic aspects of fish schooling. In Wu, T. Y. T. et al. (eds), *Swimming and Flying in Nature*. Vol. II. Plenum Press, New York, pp. 704–718.
- Wiese, K. (1996) Sensory capacities of Euphausiids in the context of schooling. *J. Mar. Freshw. Behav. Physiol.*, **28**, 183–194.
- Wiese, K. and Ebina, Y. (1995) The propulsion jet of *Euphausia superba* (Antarctic krill) as potential communication signal among conspecifics. *J. Mar. Biol. Ass. U. K.*, **75**, 43–54.
- Wiese, K. and Marschall, H. P. (1990) Sensitivity to vibration and turbulence of water in context with schooling in Antarctic Krill (*Euphausia superba*). In Wiese, K. et al. (eds), *Frontiers in Crustacean Neurobiology*. Birkhäuser-Verlag, Basel, pp. 121–130.
- Wiese, K. and Schultz, R. (1982) Intrasegmental inhibition of the displacement sensitive pathway of the crayfish (*Procambarus clarkii*). *J. Comp. Physiol.*, **147**, 447–454.
- Wiese, K., Wollnik, F. and Jebram, D. (1980) The protective reflex of *Bowerbankia* (Bryozoa): Calibration and use to indicate movement below a capillary surface wave. *J. Comp. Physiol. A*, **137**, 297–303.
- Wyse, G. A. and Maynard, D. M. (1965) Joint receptors in the antennule of *Panulirus argus* Latreille. *J. Exp. Biol.*, **42**, 521–535.
- Yen, J., Brown, J. and Webster, D. R. (2003) Analysis of the flow field of the krill *Euphausia pacifica*. *Mar. Freshw. Behav. Physiol.*, **36**, 307–319.

